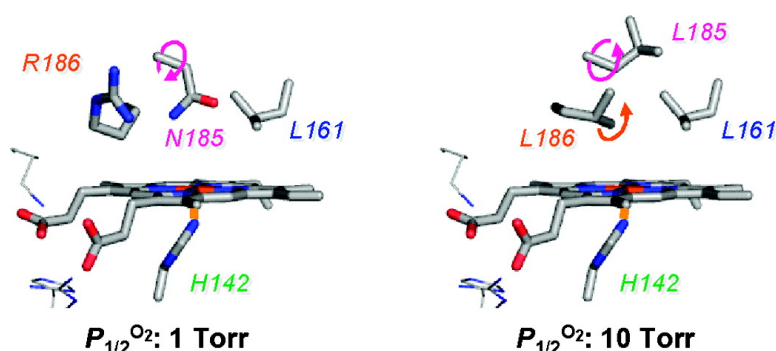


Genetic Engineering of the Heme Pocket in Human Serum Albumin: Modulation of O Binding of Iron Protoporphyrin IX by Variation of Distal Amino Acids

Teruyuki Komatsu, Akito Nakagawa, Patricia A. Zunszain, Stephen Curry, and Eishun Tsuchida

J. Am. Chem. Soc., **2007**, 129 (36), 11286-11295 • DOI: 10.1021/ja074179q • Publication Date (Web): 18 August 2007

Downloaded from <http://pubs.acs.org> on February 14, 2009



More About This Article

Additional resources and features associated with this article are available within the HTML version:

- Supporting Information
- Links to the 1 articles that cite this article, as of the time of this article download
- Access to high resolution figures
- Links to articles and content related to this article
- Copyright permission to reproduce figures and/or text from this article

[View the Full Text HTML](#)

Genetic Engineering of the Heme Pocket in Human Serum Albumin: Modulation of O₂ Binding of Iron Protoporphyrin IX by Variation of Distal Amino Acids

Teruyuki Komatsu,^{*,†,‡} Akito Nakagawa,[†] Patricia A. Zunszain,^{||} Stephen Curry,^{||} and Eishun Tsuchida^{*,†}

Contribution from the Research Institute for Science and Engineering, Waseda University, 3-4-1 Okubo, Shinjuku-ku, Tokyo 169-8555, Japan, PRESTO, Japan Science and Technology Agency, 4-1-8 Honcho, Kawaguchi-shi, Saitama 332-0012, Japan, and Division of Cell and Molecular Biology, Faculty of Natural Sciences, Imperial College London, South Kensington Campus, London SW7 2AZ, United Kingdom

Received June 8, 2007; E-mail: teruyuki@waseda.jp; eishun@waseda.jp

Abstract: Complexing an iron protoporphyrin IX into a genetically engineered heme pocket of recombinant human serum albumin (rHSA) generates an artificial hemoprotein, which can bind O₂ in much the same way as hemoglobin (Hb). We previously demonstrated a pair of mutations that are required to enable the prosthetic heme group to bind O₂ reversibly: (i) Ile-142 → His, which is axially coordinated to the central Fe²⁺ ion of the heme, and (ii) Tyr-161 → Phe or Leu, which makes the sixth coordinate position available for ligand interactions [I142H/Y161F (HF) or I142H/Y161L (HL)]. Here we describe additional new mutations designed to manipulate the architecture of the heme pocket in rHSA–heme complexes by specifically altering distal amino acids. We show that introduction of a third mutation on the distal side of the heme (at position Leu-185, Leu-182, or Arg-186) can modulate the O₂ binding equilibrium. The coordination structures and ligand (O₂ and CO) binding properties of nine rHSA(triple mutant)–heme complexes have been physicochemically and kinetically characterized. Several substitutions were severely detrimental to O₂ binding: for example, Gln-185, His-185, and His-182 all generated a weak six-coordinate heme, while the rHSA(HF/R186H)–heme complex possessed a typical bis-histidyl hemochrome that was immediately autoxidized by O₂. In marked contrast, HSA(HL/L185N)–heme showed very high O₂ binding affinity ($P_{1/2}^{O_2}$ 1 Torr, 22 °C), which is 18-fold greater than that of the original double mutant rHSA(HL)–heme and very close to the affinities exhibited by myoglobin and the high-affinity form of Hb. Introduction of Asn at position 185 enhances O₂ binding primarily by reducing the O₂ dissociation rate constant. Replacement of polar Arg-186 with Leu or Phe increased the hydrophobicity of the distal environment, yielded a complex with reduced O₂ binding affinity ($P_{1/2}^{O_2}$ 9–10 Torr, 22 °C), which nevertheless is almost the same as that of human red blood cells and therefore better tuned to a role in O₂ transport.

Introduction

In the human circulatory system, iron(III) protoporphyrin IX (hemin) released from methemoglobin (metHb) is captured by a specific glycoprotein, hemopexin (Hpx, 60 kDa), which binds it with very high affinity ($> 10^{13} \text{ M}^{-1}$).^{1,2} Nevertheless, due to the extremely low abundance of Hpx in the blood stream ($\sim 17 \mu\text{M}$), human serum albumin (HSA, 66.5 kDa, 640 μM) acts as a depot of hemin under pathological conditions of trauma and severe hemolysis.³ HSA is the most prominent plasma protein and has a remarkable ability to bind a broad range of insoluble endogenous and exogenous compounds, such as fatty acids,

hemin, bilirubin, bile acids, thyroxine, and a wide variety of drugs.^{4,5} This heart-shaped carrier protein is composed of three structurally similar domains (I–III), each of which contains two subdomains (A and B).^{6,7} Recent crystallographic studies revealed that the hemin is bound within a narrow D-shaped hydrophobic cavity in subdomain IB (Figure 1a).^{8,9} The central iron atom is weakly coordinated by Tyr-161 and the porphyrin propionate side chains interact with a triad of basic amino acid

[†] Waseda University.

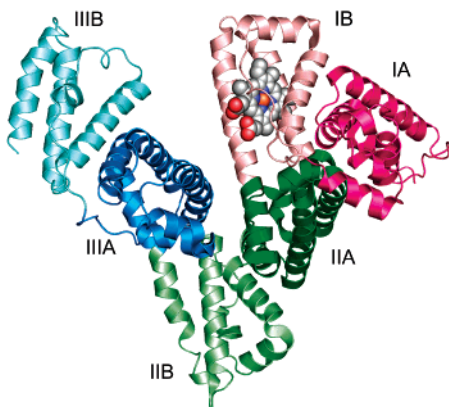
[‡] JST.

^{||} Imperial College London.

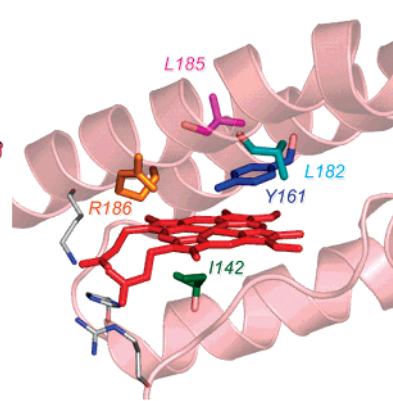
- (1) (a) Muller-Eberhard, U.; Grizzuti, K. *Biochemistry* **1971**, *10*, 2062–2066. (b) Muller-Eberhard, U.; Morgan, W. T. *Ann. N.Y. Acad. Sci.* **1975**, *244*, 624–650.
- (2) Paoli, M.; Anderson, B. F.; Baker, H. M.; Morgan, W. T.; Smith, A.; Baker, E. N. *Nat. Struct. Biol.* **1999**, *6*, 926–931.
- (3) Tolosano, E.; Altruda, F. *DNA Cell Biol.* **2002**, *21*, 297–306.

- (4) Peters, T. *All about Albumin: Biochemistry, Genetics and Medical Applications*; Academic Press: San Diego, CA, 1996; and references therein.
- (5) (a) Kragh-Hansen, U. *Pharmacol. Rev.* **1981**, *33*, 17–53. (b) Kragh-Hansen, U. *Danish Med. Bull.* **1990**, *37*, 57–84.
- (6) (a) He, X. M.; Carter, D. C. *Nature* **1992**, *358*, 209–215. (b) Carter, D. C.; Ho, J. X. *Adv. Protein Chem.* **1994**, *45*, 153–203.
- (7) (a) Curry, S.; Madelkow, H.; Brick, P.; Franks, N. *Nat. Struct. Biol.* **1998**, *5*, 827–835. (b) Bhattacharya, A. A.; Grune, T.; Curry, S. *J. Mol. Biol.* **2000**, *303*, 721–732.
- (8) Wardell, M.; Wang, Z.; Ho, J. X.; Robert, J.; Ruker, F.; Rubel, J.; Carter, D. C. *Biochem. Biophys. Res. Commun.* **2002**, *291*, 813–819.
- (9) Zunszain, P. A.; Ghuman, J.; Komatsu, T.; Tsuchida, E.; Curry, S. *BMC Struct. Biol.* **2003**, *3*, 6.

(a) HSA-hemin



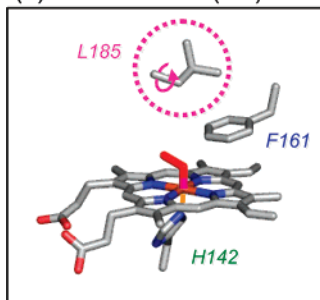
(b) Heme pocket in subdomain IB



	Positions				
	142	161	182	185	186
Wild type (wt)	I	Y	L	L	R
I142H/Y161F (HF)	H	F	L	L	R
I142H/Y161L (HL)	H	L	L	L	R
HF/L185N	H	F	L	N	R
HL/L185N	H	L	L	N	R
HF/L185Q	H	F	L	Q	R
HL/L185Q	H	L	L	Q	R
HF/L185H	H	F	L	H	R
HL/L182H	H	L	H	L	R
HF/R186H	H	F	L	L	H
HL/R186L	H	L	L	L	L
HL/R186F	H	L	L	L	F

Figure 1. (a) Crystal structure of HSA-hemin complex (1O9X) from ref 9. Hemin is shown in a space-filling representation. (b) Heme pocket structure in subdomain IB and positions of amino acids where site-specific mutations were introduced. The essential double mutations to confer O₂ binding capability to the heme group are I142H and Y161F (or Y161L). Abbreviations of the triple mutants are shown in the table.

(a) I142H/Y161F (HF)



(b) I142H/Y161L (HL)

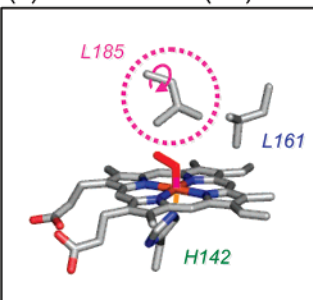


Figure 2. Structural models of the heme pocket in dioxygenated (a) rHSA(HF)-heme and (b) rHSA(HL)-heme: distal-side steric effect of Leu-185 on O₂ and CO association.²⁰

residues at the entrance (Arg-114, His-146, and Lys-190) (Figure 1b). In terms of the general hydrophobicity of the α -helical heme pocket, subdomain IB of HSA has broadly similar features to the globin-wrapping heme in Hb and myoglobin (Mb). If the HSA-based O₂ carrier is realized, it has the potential of acting not only as a red blood cell (RBC) substitute but also as an O₂-providing therapeutic reagent. However, the reduced ferrous HSA-heme would be immediately autoxidized by O₂, because HSA lacks the proximal histidine that in Hb and Mb allows the prosthetic heme group to bind O₂.¹⁰ On the basis of the detailed structure of the heme binding site of HSA, we introduced a His into the Leu-142 position by site-directed mutagenesis that provides axial coordination to the central Fe²⁺ atom of the heme, and we replaced the coordinated Tyr-161 by Phe or Leu, neither of which can interact with the Fe²⁺ ion (Figure 2).¹¹ This mutagenic approach produced the recombinant HSA(I142H/Y161F)-heme [rHSA(HF)-heme] and HSA(I142H/Y161L)-heme [rHSA(HL)-heme] complexes; these artificial hemoproteins can bind and release O₂ at room temperature, although the O₂ binding affinity of rHSA-heme is at least an order of magnitude lower than that of Hb(α) (R-state).¹¹ To develop this promising O₂-carrying plasma protein as a blood substitute,

further work is required to regulate the O₂ binding affinity suitable for Hb, Mb, and human RBC.

In Hb and Mb, His-64 on the distal side of the heme has been conserved during evolution and plays an important role for tuning their ligand affinities. A neutron diffraction study of MbO₂ clearly showed that the N-H bond of the distal His-64 is restrained from optimal alignment for strong hydrogen bonding with the coordinated O₂.¹² Olson et al.^{13a} reported that the substitution of Gly for His-64 in Mb and Hb(α) caused a significant decrease in the O₂ binding affinity due to an \sim 100-fold increase in the O₂ dissociation rate constant. A number of systematic investigations of site-directed mutants of Hb and Mb have shown that the overall polarity and packing of the distal residues are key factors in regulating the rate and equilibrium constants for ligand bindings.¹³

In addition to mutagenic analyses of heme binding sites on proteins, the value of using synthetic iron porphyrins as Hb and Mb active-site models has also been amply demonstrated.^{14,15} Tetrakis($\alpha,\alpha,\alpha,\alpha$ -*o*-pivalamido)phenylporphyrinato-iron(II) "picket-fence porphyrin" of Collman et al.¹⁶ was a pioneering molecule, which forms an O₂ adduct complex at room temperature that is quite stable and shows a high O₂ binding affinity. The polar secondary amide groups in the four fences were believed to contribute to the high O₂ affinity. Moementeau and Lavalette¹⁷ first demonstrated the distal polarity effect on the O₂ binding to the "hanging-base porphyrins". The presence of the amide groups in the strapped handle over the porphyrin macrocycle yielded a 9-fold higher O₂ binding affinity compared to the ether-bond analogue; it was due to an 8-fold reduction in the dissociation rate constant. This polarity effect of the substituent

(10) Monzani, E.; Bonafè, B.; Fallarini, A.; Redaelli, C.; Casella, L.; Minchiotti, L.; Galliano, M. *Biochim. Biophys. Acta.* **2001**, *1547*, 302–312.
 (11) (a) Komatsu, T.; Ohmichi, N.; Zunszain, P. A.; Curry, S.; Tsuchida, E. *J. Am. Chem. Soc.* **2004**, *126*, 14304–14305. (b) Komatsu, T.; Ohmichi, N.; Nakagawa, A.; Zunszain, P. A.; Curry, S.; Tsuchida, E. *J. Am. Chem. Soc.* **2005**, *127*, 15933–15942.

(12) Phillips, S. E. V.; Schoenborn, B. P. *Nature* **1981**, *292*, 81–82.
 (13) (a) Olson, J. S.; Mathews, A. J.; Rohlfs, R. J.; Springer, B. A.; Egeberg, K. D.; Sligar, S. G.; Tame, J.; Renaud, J.-P.; Nagai, K. *Nature* **1988**, *336*, 265–266. (b) Rohlfs, R.; Mathews, A. J.; Carver, T. E.; Olson, J. S.; Springer, B. A.; Egeberg, K. D.; Sligar, S. G. *J. Biol. Chem.* **1990**, *265*, 3168–3176. (c) Springer B. A.; Sligar, S. G.; Olson, J. S.; Phillips, G. N., Jr. *Chem. Rev.* **1994**, *94*, 699–714.
 (14) Moementeau, M.; Reed, C. A. *Chem. Rev.* **1994**, *94*, 659–698.
 (15) Collman, J. P.; Fu, L. *Acc. Chem. Res.* **1999**, *32*, 455–463.
 (16) (a) Collman, J. P.; Gagne, R. R.; Halbert, T. R.; Marchou, J.-C.; Reed, C. A. *J. Am. Chem. Soc.* **1973**, *95*, 7869–7870. (b) Collman, J. P.; Gagne, R. R.; Reed, C. A.; Halbert, T. R.; Lang, G.; Robinson, W. T. *J. Am. Chem. Soc.* **1975**, *97*, 1427–1439. (c) Collman, J. P.; Brauman, J. I.; Iverson, B. L.; Sessler, J. L.; Morris, R. M.; Gibson, Q. H. *J. Am. Chem. Soc.* **1983**, *105*, 3052–3064.
 (17) Moementeau, M.; Lavalette, D. *J. Chem. Soc., Chem. Commun.* **1982**, 341–343.

was also well illustrated by our “double-sided porphyrins” having ester fences with a 23-fold lower O₂ binding affinity relative to the picket-fence porphyrin.¹⁸

In view of these investigations, we reasoned that systematic variation of the steric hindrance and local polarity of the heme pocket in subdomain IB of HSA would allow us to modulate the O₂ binding affinity of rHSA–heme. In this study, we designed and generated nine rHSA(triple mutant)–heme complexes, in which the specific third mutation was introduced into three different positions near the O₂ binding site. The effects of the engineered distal amino acids on the O₂ and CO binding properties of the prosthetic heme group have been physico-chemically and kinetically characterized. We now present a new chemistry of albumin-based artificial hemoproteins that would serve as an entirely synthetic O₂ carrier with a controllable ligand binding affinity.

Experimental Section

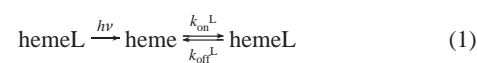
Materials and Apparatus. All materials were reagent-grade and were used as purchased without further purification. Iron(III) protoporphyrin IX (hemin) chloride was purchased from Fluka. UV–vis absorption spectra were obtained on an Agilent 8453 UV–visible spectrophotometer equipped with an Agilent 89090A temperature control unit. Kinetic measurements for the O₂ and CO bindings were carried out on a Unisoku TSP-1000WK time-resolved spectrophotometer with a Spectron Laser Systems SL803G-10 Q-switched Nd:YAG laser, which generated a second-harmonic (532 nm) pulse of 6-ns duration (10 Hz).^{11b} A 150 W xenon arc lamp was used as the probe light source. The gas mixture with the desired partial pressure of O₂/CO/N₂ was prepared by a Kofloc Gasblender GB-3C. MCD spectra were measured by a Jasco J-820 circular dichrometer.

Preparations of rHSA Triple Mutants and Their Heme Complexes. The designed rHSA triple mutants were prepared according to our previously reported techniques.¹¹ The third mutation (L185N, L185Q, L185H, L182H, R186H, R186L, or R186F) was introduced into the HSA coding region in a plasmid vector encoding the double mutants [rHSA(I142H/Y161F) [rHSA(HF)] or rHSA(I142H/Y161L) [rHSA(HL)]]¹¹ by use of the Stratagene QuikChange mutagenesis kit. All mutations were confirmed by DNA sequencing. The plasmid was then digested by *NotI* and introduced into yeast (*Pichia pastoris* GS115) by electroporation. The expression protocols and media formulations were as previously described.^{11b} Briefly, the clones were grown in BMGY medium and transferred to BMMY medium for induction with methanol in baffled shaking flasks at 30 °C, 200 rpm. The obtained proteins were harvested from the growth medium by precipitation with ammonium sulfate and purified by a Cibacron Blue column of Blue Sepharose 6 Fast Flow (Amersham Pharmacia Biotech). The rHSA triple mutants were finally subjected to gel filtration on an ÄKTA Prime Plus FPLC system with a Superdex 75 preparative-grade column (Amersham Pharmacia Biotech). The protein concentration was assayed by measuring the absorbance at 280 nm ($\epsilon_{280} = 3.4 \times 10^4 \text{ M}^{-1} \text{ cm}^{-1}$) and by SDS–PAGE.

The ferric rHSA(mutant)–hemin complexes [hemin:rHSA(mutant) molar ratio of 1:1] were prepared by established procedures.^{9,11} The resulting samples were analyzed by SDS–PAGE to confirm a pure preparation. The 50 mM phosphate buffered solution (pH 7.0, 3 mL) of rHSA(mutant)–hemin ([hemin] = 10 μM) in a 10-mm path length optical quartz cuvette sealed with a rubber septum was purged with Ar for 40 min. A small excess amount of degassed aqueous sodium dithionate was added by a microsyringe to the sample under an Ar

atmosphere to reduce the central ferric ion of the heme, to give the ferrous rHSA(mutant)–heme complexes.

O₂ and CO Binding Parameters. The O₂ or CO recombination with the heme after nanosecond laser flash photolysis of hemeO₂ or hemeCO occurs according to eq 1 with the association rate constant (k_{on}^{L}) and dissociation rate constant ($k_{\text{off}}^{\text{L}}$):^{11,16c,19}



where L = O₂ or CO. The CO association rate ($k_{\text{on}}^{\text{CO}}$) was simply measured by following the absorption at 425 nm after laser pulse irradiation to rHSA(mutant)–hemeCO at 22 °C.¹¹ The O₂ association rate constant ($k_{\text{on}}^{\text{O}_2}$) and O₂ binding equilibrium constant K^{O_2} [$= (P_{1/2}^{\text{O}_2})^{-1}$] can be determined by a competitive rebinding technique by use of gas mixtures with different partial pressures of O₂/CO/N₂ at 22 °C.^{11,16c,19} The relaxation curves that accompanied the O₂ or CO recombination were analyzed by single- or double-exponential profiles with Unisoku Spectroscopy & Kinetics software. The O₂ dissociation rate ($k_{\text{off}}^{\text{O}_2}$) was calculated from $k_{\text{on}}^{\text{O}_2}/K^{\text{O}_2}$.

The CO dissociation rate constant ($k_{\text{off}}^{\text{CO}}$) was measured by displacement with NO for rHSA(mutant)–hemeCO at 22 °C.^{11b} The time course of the UV–vis absorption change that accompanied the CO dissociation was fitted to two single exponentials. The CO binding constants [$K^{\text{CO}} = (P_{1/2}^{\text{CO}})^{-1}$] were calculated from $k_{\text{on}}^{\text{CO}}/k_{\text{off}}^{\text{CO}}$. Fresh solutions of rHSA–(mutant)–heme were normally made up for each set of experiments.

Magnetic Circular Dichroism Spectroscopy. MCD for the 50 mM potassium phosphate buffered solutions (pH 7.0) of rHSA(mutant)–hemin or –heme complex (10 μM) were measured under Ar and CO atmospheres with a 1.5 or 1.65 T electromagnet at 22 °C.

Results and Discussion

Design of Distal Pocket with Asn, Gln, and His. We recently compared the O₂ and CO binding properties of the rHSA(double mutant)–heme complexes [rHSA(HF)–heme and rHSA(HL)–heme] and found evidence for a noteworthy distal-side steric effect on ligand binding.^{11b} The rHSA(HF)–heme complex binds O₂ and CO about 4–6 times more tightly than rHSA(HL)–heme, primarily because of enhanced association rate constants. Structurally, this affect appears to be due to the concerted effects of the residues at positions 161 and 185 on ligand binding. In the rHSA(HF)–heme complex, the bulky aromatic side chain of Phe-161 is presumed to prevent rotation of the neighboring Leu-185, thereby providing easy access to the O₂ binding site in the distal pocket (Figure 2a). In contrast, the substitution of Phe-161 by the smaller Leu-161 may allow rotation of the isopropyl group of Leu-185, which reduces the volume of the distal side (Figure 2b) and hinders association of O₂ and CO ligands with the heme iron atom. On the basis of these findings, we reasoned that other modifications of the heme pocket architecture would allow us to further modulate its O₂ binding properties.

One approach to enhancing the O₂ binding affinities of rHSA–(HF)–heme and rHSA–(HL)–heme would be to introduce a histidine into an appropriate position on the distal side of the heme. The N_ε atom of His may act as a proton donor to form an H-bond with the coordinated O₂. However, another important requirement in this molecular design is to prevent the formation

(18) (a) Komatsu, T.; Hasegawa, E.; Nishide, H.; Tsuchida, E. *J. Chem. Soc., Chem. Commun.* **1990**, 66–68. (b) Tsuchida, E.; Komatsu, T.; Arai, K.; Nishide, H. *J. Chem. Soc., Dalton Trans.* **1993**, 2465–2469.

(19) Traylor, T. G.; Tsuchiya, S.; Campbell, D.; Mitchel, M.; Stynes, D.; Koga, N. *J. Am. Chem. Soc.* **1985**, *107*, 604–614.

(20) The pictures were produced on the basis of crystal structure coordinates of rHSA(wt)–hemin (1O9X, ref 9) by use of PyMOL: DeLano, W. L. The PyMOL Molecular Graphics System; DeLano Scientific: San Carlos, CA, 2002.

of a six-coordinate low-spin ferrous complex. The bis-histidyl hemochromes are normally autoxidized by O₂ via an outer-sphere mechanism as well as by inner-sphere pathways involving the metal-coordinated O₂.^{21–23} The distal amino acid must therefore be located relatively far (>4 Å) from the central iron.

Our modeling experiments suggested that the favorable position for the distal His insertion was Leu-185, which is in the final helix in subdomain IB and forms part of the top of the distal pocket (Figure 1). Leu-182 and Arg-186 were also considered likely to be good candidate positions for the introduction of an amide-containing side chain designed to stabilize O₂ binding (see below). In elegant studies on Mb, Rohlfs and co-workers showed that Gln, which has a primary amide group potential to form an H-bond, was able to substitute effectively for the stabilizing role of the distal histidine (His-64).^{13b,c} Thus, we decided to vary the polarity of the distal side of the heme in rHSA(HF) and rHSA(HL) by replacing Leu-185 with Asn, Gln, and His by site-directed mutagenesis. The Asn residue should behave similarly to Gln, although a rMb-(H64N) mutant has never been reported. The His-185 mutation was only done for rHSA(HF), because His-185 could be long enough to bind to the sixth coordinate position of the heme if allowed the greater freedom of movement that would occur in the rHSA(HL) background. As a result, five triple mutants [rHSA(HF/L185N), rHSA(HL/L185N), rHSA(HF/L185Q), rHSA(HL/L185Q), and rHSA(HF/L185H)] were cloned and their hemin complexes were prepared.

Ferric States of L185N, L185Q, and L185H Mutants. The site-specific mutations with Asn, Gln, and His were successfully introduced into the Leu-185 position of rHSA(HF) or rHSA(HL), and the proteins were purified to homogeneity as determined by SDS–PAGE. The rHSA(mutant)–hemin complexes produced from these proteins were stable for several months at 4 °C without precipitation.

The UV–vis absorption spectra of the five rHSA(triple mutant)–hemin complexes are essentially the same regarding their general features (Figure 3, Table 1). When analyzed by MCD spectroscopy to evaluate the redox state, spin state, and axial ligand environment, all the ferric rHSA(triple mutant)–hemins showed a characteristic MCD with similar S-shaped patterns in the Soret band region, though their intensities were dependent on the nature of the distal amino acid (Figure 4). Vickery et al.²⁴ previously reported that the Soret MCD intensity of the ferric Mb with different anions at the sixth coordinate position was correlated with the amount of low-spin component. rHSA(HL)–hemin showed almost the same band as ferric Mb, in which one water axially coordinates to the sixth position of the heme to produce the aquo complex.^{11,24,25} In contrast, rHSA(HF/L185H)–hemin showed 3-fold greater intensity at 405 nm. This is probably caused by the coexistence of a low-spin six-coordinate heme. Introduction of Asn or Gln at position 185

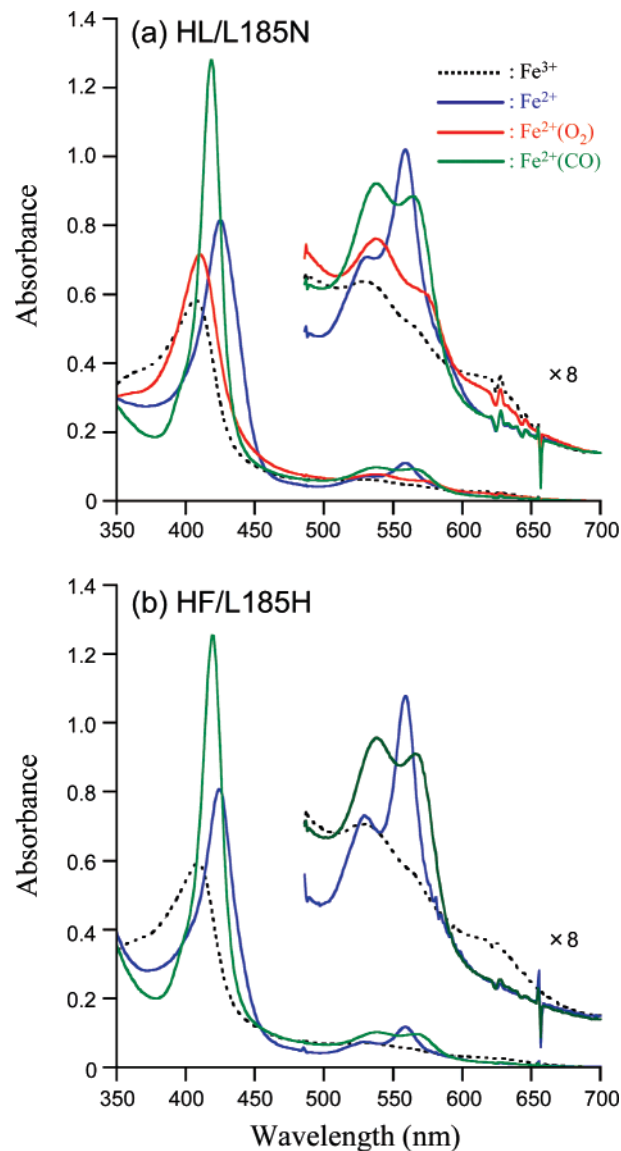


Figure 3. UV–vis absorption spectral changes of (a) rHSA(HL/L185N)–heme and (b) rHSA(HF/L185H)–heme complexes in 50 mM potassium phosphate buffered solution (pH 7.0, 22 °C).

gave intermediate effects, though mutants with Q185 yielding a slightly more intense peak at 405 nm. Overall, our MCD results for these five rHSA(triple mutant)–hemins imply that the introduction of the distal nitrogenous residue at the 185 position tends to increase the ferric low-spin nature.

Ferrous States of L185N, L185Q, and L185H Mutants and O₂ Binding. rHSA(triple mutant)–hemins were easily reduced to form the ferrous complexes by adding a small excess of aqueous sodium dithionite under an Ar atmosphere. rHSA(HF/L185N)–heme, rHSA(HL/L185N)–heme, and rHSA(HL/L185Q)–heme each showed a visible absorption band at 558–559 nm with a small shoulder at 530 nm (Figure 3a; Figure S1, Supporting Information), that was similar to the spectra observed for rHSA(HF)–heme, rHSA(HL)–heme,^{11b} deoxyMb,²⁷ and synthetic chelated protoheme.²⁶ The spectral patterns clearly indicated the formation of a five-N-coordinate high-spin complex. In contrast, in the spectra of rHSA(HF/L185Q)–heme and

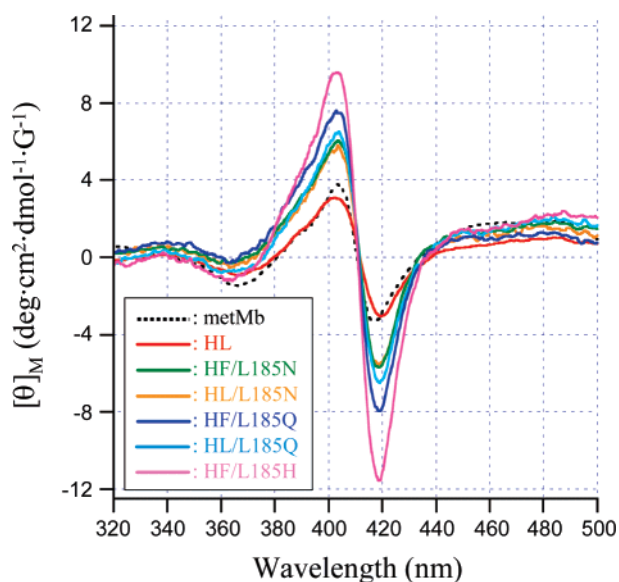
- (21) Chu, M. M. L.; Castro, C. E.; Hathaway, G. M. *Biochemistry* **1978**, *17*, 481–486.
 (22) Tsuchida, E.; Nishide, H.; Sato, Y.; Kaneda, M. *Bull. Chem. Soc. Jpn.* **1982**, *55*, 1890–1895.
 (23) Uno, T.; Sakamoto, R.; Tomisugi, Y.; Ishikawa, Y.; Wilkinson, A. *Biochemistry* **2003**, *42*, 10191–10199.
 (24) Vickery, L.; Nozawa, T.; Sauer, K. *J. Am. Chem. Soc.* **1976**, *98*, 343–350.
 (25) Collman, J. P.; Basolo, F.; Bunnenberg, E.; Collins, T. J.; Dawson, J. H.; Ellis, P. E., Jr.; Marrocco, M. L.; Moscovitz, A.; Sessler, J. L.; Szymanski, T. *J. Am. Chem. Soc.* **1981**, *103*, 5636–5648.
 (26) Traylor, T. G.; Chang, C. K.; Geibel, J.; Berzins, A.; Mincey, T.; Cannon, J. *J. Am. Chem. Soc.* **1979**, *101*, 6716–6731.

- (27) Antonini, E.; Brunori, M. *Hemoglobin and Myoglobin in Their Reactions with Ligands*; North-Holland: Amsterdam, 1971; p 18.

Table 1. UV–vis Absorption Spectral Data of rHSA(mutant)–Heme Complexes^a

hemoproteins	λ_{max} (nm)			
	Fe ³⁺	Fe ²⁺	Fe ²⁺ O ₂	Fe ²⁺ CO
rHSA(HF)–heme ^b	402, 533, 620	425, 532(sh), 559	411, 538, 576	419, 538, 565
rHSA(HL)–heme ^b	402, 533, 620	426, 531(sh), 559	412, 537, 573	419, 538, 565
rHSA(HF/L185N)–heme	406, 528, 618	425, 530(sh), 559	411, 540, 575	419, 539, 566
rHSA(HL/L185N)–heme	407, 530, 620	425, 530(sh), 559	411, 537, 575	419, 537, 564
rHSA(HF/L185Q)–heme	406, 530, 620	424, 528, 558		419, 538, 566
rHSA(HL/L185Q)–heme	406, 530, 620	425, 530(sh), 558	411, 537, 574 ^c	419, 537, 566
rHSA(HF/L185H)–heme	407, 528, 620	424, 528, 558		419, 538, 566
rHSA(HL/L182H)–heme	410, 532, 624	425, 530, 559		419, 539, 567
rHSA(HF/R186H)–heme	411, 533, 565	424, 529, 560		420, 539, 568
rHSA(HL/R186L)–heme	406, 530, 620	426, 531(sh), 559	411, 539, 576	419, 539, 567
rHSA(HL/R186F)–heme	405, 532, 621	426, 531(sh), 559	410, 535, 571	419, 538, 568
Mb ^d	409, 503, 548(sh), 632	434, 557	418, 544, 581	423, 541, 579
chelated heme ^e	408, 540, 565	427, 530, 558	414, 543, 575	420, 540, 569

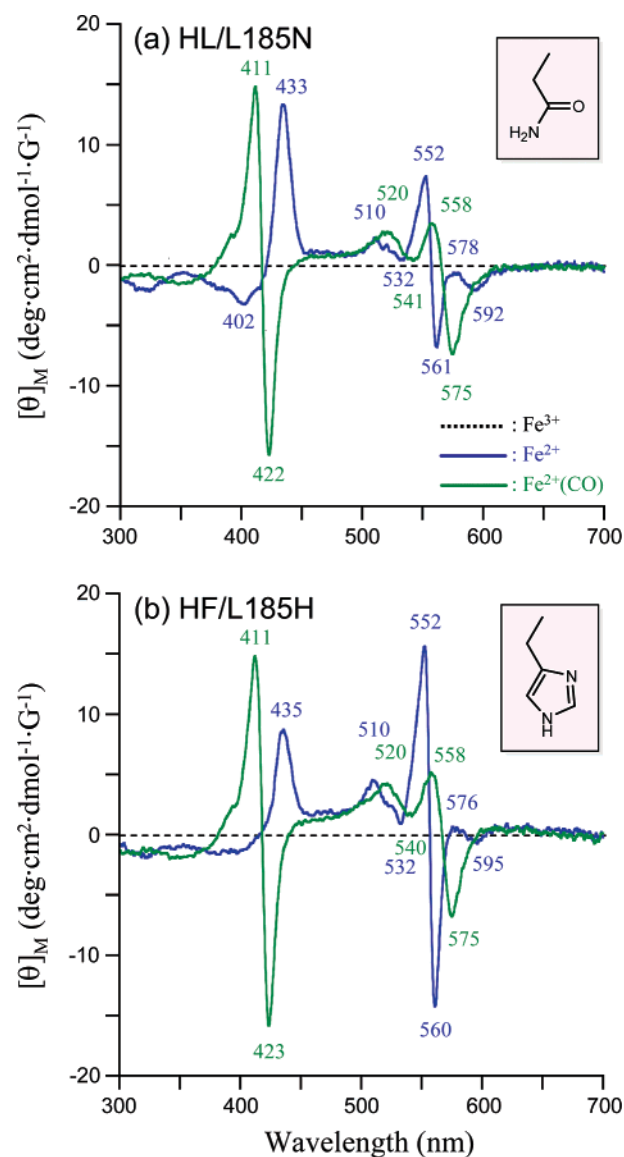
^a In 50 mM potassium phosphate buffered solution (pH 7.0) at 22 °C. ^b Reference 11b. ^c At 5 °C. ^d Horse muscle myoglobin (Sigma); ref 11b. ^e In DMF/H₂O (7/3) at 15 °C; ref 26.

**Figure 4.** MCD spectra of rHSA(185-mutant)–hemin complexes in 50 mM potassium phosphate buffered solution (pH 7.0, 22 °C).

rHSA(HF/L185H)–heme, the β band at 528 nm appeared relatively sharp (Figure 3b), which suggests partial formation of a six-coordinate heme complex. This is consistent with the finding that the ferric state of these two mutant complexes had the highest peaks in the MCD.

The Soret MCD spectra of ferrous rHSA(HF/L185N)–heme, rHSA(HL/L185N)–heme, and rHSA(HL/L185Q)–heme under Ar atmosphere are dominated by an intense positive peak at 433 nm and a small trough at 402 nm as expected for the Faraday C-terms for high-spin ferrous porphyrins like deoxyMb (Figure 5a).^{24,25} In contrast to these three mutant complexes, rHSA(HF/L185Q)–heme and rHSA(HF/L185H)–heme show weaker intensity in the Soret band region and greater intensity in the visible region (Figure 5b).

On the basis of all the UV–vis absorption and MCD spectral results, we concluded that the reduced ferrous heme is axially coordinated by His-142 at the core of the heme pocket in rHSA-(mutant) and forms a five-N-coordinate high-spin ferrous complex under an Ar atmosphere in the case of HF/L185N, HL/L185N, and HL/L185Q mutants (Figure 6a,b,d). In addition to the His-142 ligation, Gln-185 and His-185 partially interact with the sixth coordinate position of the central Fe²⁺ ion of the

**Figure 5.** MCD spectral changes of (a) rHSA(HL/L185N)–heme and (b) rHSA(HF/L185H)–heme complexes in 50 mM potassium phosphate buffered solution (pH 7.0, 22 °C).

heme in the HF/L185Q and HF/L185H mutants in spite of the bulky aromatic ring of Phe-161 (Figure 6c,e). We postulated that rHSA(HL/L185Q)–heme would also form a six-coordinate

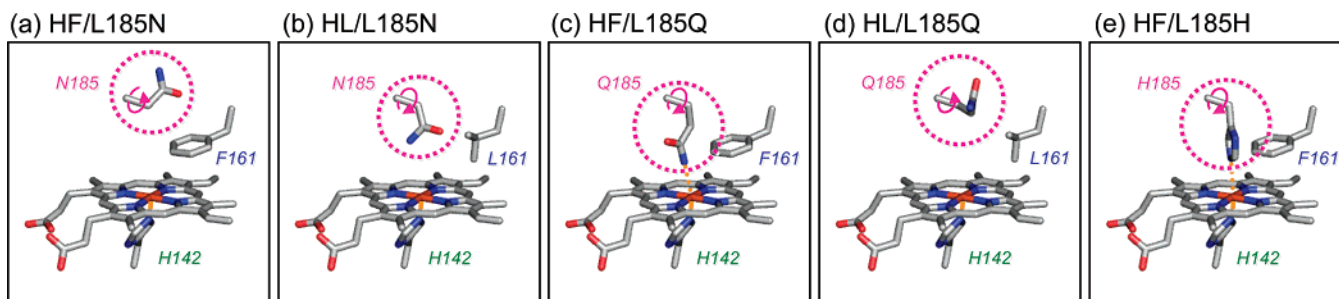


Figure 6. Structural models of the heme pocket in rHSA(triple mutant)-heme complexes: distal-side effects of engineered amino acids at position 185.

low-spin complex, because the small Leu-161 should allow additional room for rotation of Gln-185. However, it yielded a five-coordinate high-spin ferrous complex (Figure S1). This suggests that the flexible Gln-185 may interact with neighboring amino acids (Figure 6d) and underscores the difficulty in accurately predicting the impact of amino acid substitutions.

Upon exposure of the rHSA(HF/L185N)-heme and rHSA(HL/L185N)-heme solutions to O₂, the UV-vis absorptions immediately changed to that of the O₂ adduct complex at 22 °C (Figure 3a, Table 1).^{11,26,27} However, the rHSA(HL/L185Q)-heme complex bound O₂ only at 5 °C (Figure S1a) and was observed to autoxidize rapidly at 22 °C. This rapid oxidation may suggest that the distal side of the heme has an open structure, which allows easy access of water to the heme, thereby facilitating autoxidation.²⁸ The rHSA(HF/L185Q)-heme and rHSA(HF/L185H)-heme complexes, both of which exhibit side-chain interactions with the sixth coordinate position of the heme, were immediately oxidized by O₂ even at low temperature (5 °C).

After introduction of CO gas, all the hemoproteins produced stable carbonyl complexes with identical absorption spectral patterns (Figures 3 and S1a, Table 1).^{11,26,27} In every case the carbonyl rHSA(triple mutant)-heme complexes exhibited the same S-shaped MCDs, which correspond to the A-term bands for the diamagnetic low-spin protoheme with CO and axial His coordinations (Figures 5 and S1b).^{24,25} This result implies that in the carbonyl complexes the Asn-185 and Gln-185 residues do not act as a proximal base instead of His-142.

O₂ and CO Binding Parameters of L185N Mutants. By use of laser flash photolysis, analysis of the kinetics of ligand binding to the double mutants rHSA(HF)-heme and rHSA(HL)-heme revealed that the asymmetric iron protoporphyrin IX molecule is accommodated in subdomain IB in two different orientations (180° rotational isomers).¹¹ As a result, there exist two geometries of the axial His-142 coordination to the central Fe²⁺ ion of the heme (species I and II). In species I, the proximal His coordinates to the heme without strain, while in species II, the ligation involves some distortion, resulting in weaker O₂ binding. The bending strain in the proximal His-Fe²⁺ bond in species II increases the dissociation rate constant and decreases the association rate for CO, whereas it increases the O₂ dissociation rate without changing the kinetics of the O₂ association.^{16c,19} Consequently, the entire absorption decay accompanying the CO recombination with rHSA(HF)-heme or rHSA(HL)-heme was composed of two single exponentials, but the rebinding process of O₂ followed a simple monophasic

decay. In rHSA(triple mutant)-hememes, this alternative geometry of the heme plane would also arise in the same manner.

We again used laser flash photolysis to characterize the O₂ and CO binding properties of the rHSA(triple mutant)-heme complexes. As expected, the binding behavior of O₂ for rHSA(HF/L185N)-heme and rHSA(HL/L185N)-heme was broadly similar to that of the double mutants. However, detailed analysis reveals that the absorption decay accompanied by O₂ rebinding to the heme was composed of two very similar phases (Figure S2, Supporting Information). Numerous investigations of the synthetic iron porphyrins have demonstrated that the “distal-side steric effect” is the only factor that influences the association rate constant for O₂.^{16c,19} The double-exponential profiles for O₂ association are therefore likely to indicate that there are two distinct conformations of the distal Asn-185 above the heme. The amplitude ratio of the two phases was approximately 1:1 for rHSA(HL/L185N)-heme, suggesting that half of the Asn residue may turn toward the inside of the heme pocket and the other turns to the outside (Figure 6b). These two conformers of the distal Asn-185 residue also influence the association rate for CO. If we were to take this minimal effect into account, the CO rebinding process would have to be analyzed as four phases. However, (i) it would be too complicated to comprehend the fundamental aspects of the ligand binding properties of rHSA(triple mutant)-heme, and (ii) the observed distal-side effect is less significant compared to the major proximal-side steric effect in this system. Hence, the absorbance decays after laser pulse irradiation to rHSA(HF/L185N)-hemeCO and rHSA(HL/L185N)-hemeCO were fitted by biphasic kinetics. The ratio of the amplitude of the dominant fast phase (species I) and minor slow phase (species II) was approximately 7:3 for rHSA(HF/L185N)-heme and 3:2 for rHSA(HL/L185N)-heme. These values were within the same range observed in the rHSA(double mutant)-heme complexes.¹¹ Concomitantly, the O₂ association rate of rHSA(HF/L185N)-heme or rHSA(HL/L185N)-heme was determined as one value by weighted averaging of the $k_{\text{on}}^{\text{O}_2}$ values for the two phases (Table 2).

In general, $k_{\text{off}}^{\text{CO}}$ is a simple indicator of the bending strain in the proximal His coordination to the central Fe²⁺ ion.^{16c,19} rHSA(HF)-heme, rHSA(HL)-heme, rHSA(HF/L185N)-heme, and rHSA(HL/L185N)-heme exhibited similar $k_{\text{off}}^{\text{CO}}$ values in species I (0.008–0.013 s⁻¹) and they are identical to that of Hb(α) (R-state) (0.009 s⁻¹) (Table 3).²⁹ This result indicated that the axial His-142 ligation to the heme in these artificial hemoproteins has the same features as that of Hb.

(28) Brantley, R. E., Jr.; Smerdon, S. J.; Wilkinson, A. J.; Singleton, E. W.; Olson, J. S. *J. Biol. Chem.* **1993**, *268*, 6995–7010.

(29) Sharma, V. S.; Schmidt, M. R.; Ranney, H. M. *J. Biol. Chem.* **1976**, *251*, 4267–4272.

Table 2. O₂ Binding Parameters of rHSA(mutant)–Heme Complexes^a

hemoproteins	$k_{\text{on}}^{\text{O}_2}$ ($\mu\text{M}^{-1} \text{s}^{-1}$)	$k_{\text{off}}^{\text{O}_2}$ (ms^{-1})		$P_{1/2}^{\text{O}_2}$ (Torr)	
		I	II	I	II
rHSA(HF)–heme ^b	20	0.10	0.99	3	31
rHSA(HL)–heme ^b	7.5	0.22	1.70	18	134
rHSA(HF/L185N)–heme	26	0.10	1.03	2	24
rHSA(HL/L185N)–heme	14	0.02	0.29	1	14
rHSA(HL/R186L)–heme	25	0.41	8.59	10	209
rHSA(HL/R186F)–heme	21	0.29	7.01	9	203
Hb(α) (R-state) ^c	33 ^d	0.013 ^e		0.24	
Mb ^f	14	0.012		0.51	
RBC ^g				8	

^a In 50 mM potassium phosphate buffered solution (pH 7.0) at 22 °C. I or II indicates species I or II. ^b Reference 11. ^c Human hemoglobin α -subunit. ^d In 0.1 M phosphate buffer (pH 7.0, 21.5 °C); ref 30. ^e In 10 mM phosphate buffer (pH 7.0, 20 °C); ref 31. ^f Sperm whale myoglobin, in 0.1 M potassium phosphate buffer (pH 7.0, 20 °C); ref 13b. ^g Human red cell suspension, in isotonic buffer (pH 7.4, 20 °C); ref 32.

Table 3. CO Binding Parameters of rHSA(mutant)–Heme Complexes^a

hemoproteins	$k_{\text{on}}^{\text{CO}}$ ($\mu\text{M}^{-1} \text{s}^{-1}$)		$k_{\text{off}}^{\text{CO}}$ (s^{-1})		$P_{1/2}^{\text{CO}}$ (Torr)	
	I	II	I	II	I	II
rHSA(HF)–heme ^b	6.8	0.72	0.009	0.061	0.0011	0.068
rHSA(HL)–heme ^b	2.0	0.27	0.013	0.079	0.0053	0.240
rHSA(HF/L185N)–heme	7.7	1.09	0.008	0.043	0.0008	0.032
rHSA(HL/L185N)–heme	6.8	1.60	0.008	0.039	0.0010	0.020
rHSA(HL/R186L)–heme	5.0	0.57	0.011	0.165	0.0018	0.234
rHSA(HL/R186F)–heme	7.9	1.12	0.010	0.148	0.0010	0.107
Hb(α) (R-state) ^c	4.6 ^d		0.009 ^e		0.0016 ^f	
Mb ^g	0.51		0.019		0.030	

^a In 50 mM potassium phosphate buffered solution (pH 7.0) at 22 °C. I or II indicates species I or II. ^b Reference 11. ^c Human hemoglobin α -subunit. ^d In 50 mM potassium phosphate buffer (pH 7.0, 20 °C); ref 33. ^e In 0.1 M phosphate buffer (pH 7.0, 20 °C); ref 29. ^f Calculated from $(k_{\text{on}}^{\text{CO}}/k_{\text{off}}^{\text{CO}})^{-1}$. ^g Sperm whale myoglobin, in 0.1 M potassium phosphate buffer (pH 7.0, 20 °C); ref 13b.

Effect of Asn-185 Residue on O₂ Binding Affinity. The O₂ and CO binding parameters for the rHSA(HF)–heme and rHSA(HF/L185N)–heme complexes did not show any significant differences. The bulky benzyl side chain of Phe-161 may retard rotation of the polar amide group of Asn-185 and thereby maintain the polarity and size of the distal pocket (Figure 6a). In contrast, there are marked differences in the comparison of the O₂ and CO binding parameters for rHSA(HL)–heme and rHSA(HL/L185N)–heme. First, the presence of Asn rather than Leu at position 185 resulted in 2- and 3–6-fold increases in the association rate constants for O₂ and CO, respectively. As described above, the kinetics of O₂ binding to rHSA(HL/L185N)–heme actually consist of two phases. The Asn may partly rotate upward, which provides a somewhat greater space for the distal pocket. This presumably increases the association rate constants. Second, Asn-185 induced 18- and 10-fold increases in the O₂ binding affinity for species I and II, respectively (Table 2); these increases were predominantly due to the 6–11-fold diminution of the $k_{\text{off}}^{\text{O}_2}$ values. This corresponds to a free energy difference of $-1.8 \text{ kcal mol}^{-1}$ at 22 °C that may be attributable to a H-bond interaction with the bound O₂. This is consistent with the observation that, in HbO₂ and MbO₂, the distal His-64 stabilizes the coordinated O₂ by $-0.6 \sim -1.4 \text{ kcal mol}^{-1}$ due to the H-bonding.¹³ Unfortunately, attempts to measure the stretching frequency of the bound O₂ molecule in rHSA(HL/L185N)–heme by infrared spectroscopy failed because the O₂ adduct complex was not sufficiently stable.

Nevertheless, it is noteworthy that the high O₂ binding affinity ($P_{1/2}^{\text{O}_2}$ 1 Torr) for rHSA(HL/L185N)–heme is now close to that of natural Hb(α) (0.24 Torr)^{30,31} and Mb (0.5 Torr)¹³ (Table 2).

Replacement of L182 or R186 by His. Leu-182 and Arg-186 were also considered to be good candidates for introduction of the distal His, so we prepared the rHSA(HL/L182H) and rHSA(HF/R186H) triple mutants (Figure 1). Modeling trials demonstrated that neither of these introduced histidines is coplanar with the Fe–O–O moiety. Rather, they are positioned off to the side, so that there may be an oblique interaction with the coordinated O₂ and the heme center.

The rHSA(HL/L182H)–hemin complex and its reduced form showed spectra similar to those of rHSA(HF/L185H)–heme. In contrast, the color of the ferric rHSA(HF/R186H)–hemin solution was bright red, and the UV–vis absorption spectrum clearly showed the formation of a bis-histidine-coordinated low-spin ferric complex (Figure 7a).^{22,26} The MCD intensity of the S-shaped curve in the Soret band region (Figure 8) was higher than that observed with rHSA(HF/L185H)–hemin (Figure 4). The chemical reduction of the Fe³⁺ complex results in very sharp β , α bands in the visible absorption spectrum (529, 560 nm) (Figure 7a). In MCD, we observed the loss of the strong C-terms in the Soret band and the appearance of intense A-terms corresponding to the α band (Figure 7b). They all resembled those of the typical bis-histidyl hemochrome, for example, cytochrome *b*₅,³⁴ soluble guanylcyclase,^{35a} and bis-imidazole-bound protoheme,^{22,26,35b} as well as Hpx.^{1b} It can be concluded that rHSA(HF/R186H)–heme produced a strong six-coordinate low-spin ferrous complex under an Ar atmosphere. Unfortunately, the ferrous forms of both rHSA(HF/R186H)–heme and rHSA(HL/L182H)–heme were readily autoxidized upon the addition of O₂ gas. It is known that bis-histidyl hemochromes are rapidly oxidized by O₂ via an outer-sphere mechanism.²¹ We have demonstrated that this also applies to our artificial hemoprotein, the rHSA(mutant)–heme system.

O₂ and CO Binding Parameters for R186L and R186F Mutants. We have clearly shown that the O₂ binding equilibrium and kinetics of rHSA–heme complexes may be significantly enhanced by site-directed mutagenesis. In fact, the O₂ binding affinity of the rHSA(HL/L185N)–heme complex (1 Torr) was shown to be similar to those of Mb and the high-affinity R-state of Hb(α). However, for saline solutions of artificial rHSA–heme complexes to provide effective lung-to-tissue O₂ transport in vivo, the affinity should be reduced to render it more similar to the affinity of human RBC ($P_{1/2}^{\text{O}_2}$ 8 Torr).³² This requires an O₂ binding affinity that is intermediate between the values observed for rHSA(HL)–heme and rHSA(HL/L185N)–heme.

Both site-directed mutagenesis and synthetic porphyrin approaches have previously shown that an effective way to diminish the O₂ binding affinity of the heme is to introduce a

- (30) Gibson, Q. H. *J. Biol. Chem.* **1970**, *245*, 3285–3288.
 (31) Olson, J. S.; Andersen, M. E.; Gibson, Q. H. *J. Biol. Chem.* **1971**, *246*, 5919–5923.
 (32) Imai, K.; Morimoto, H.; Kotani, M.; Watari, H.; Hirata, W.; Kuroda, M. *Biochim. Biophys. Acta.* **1970**, *200*, 189–197.
 (33) Steinmeier, R. C.; Parkhurst, L. J. *Biochemistry* **1975**, *14*, 1564–1571.
 (34) Vickery, L.; Salmon, A.; Sauer, K. *Biochim. Biophys. Acta.* **1975**, *386*, 87–98.
 (35) (a) Burstyn, J. N.; Yu, A. E.; Dierks, E. A.; Hawkins, B. K.; Dawson, J. H. *Biochemistry* **1995**, *34*, 5896–5903. (b) Svastits, E. W.; Dawson, J. H. *Inorg. Chim. Acta.* **1986**, *123*, 83–86.

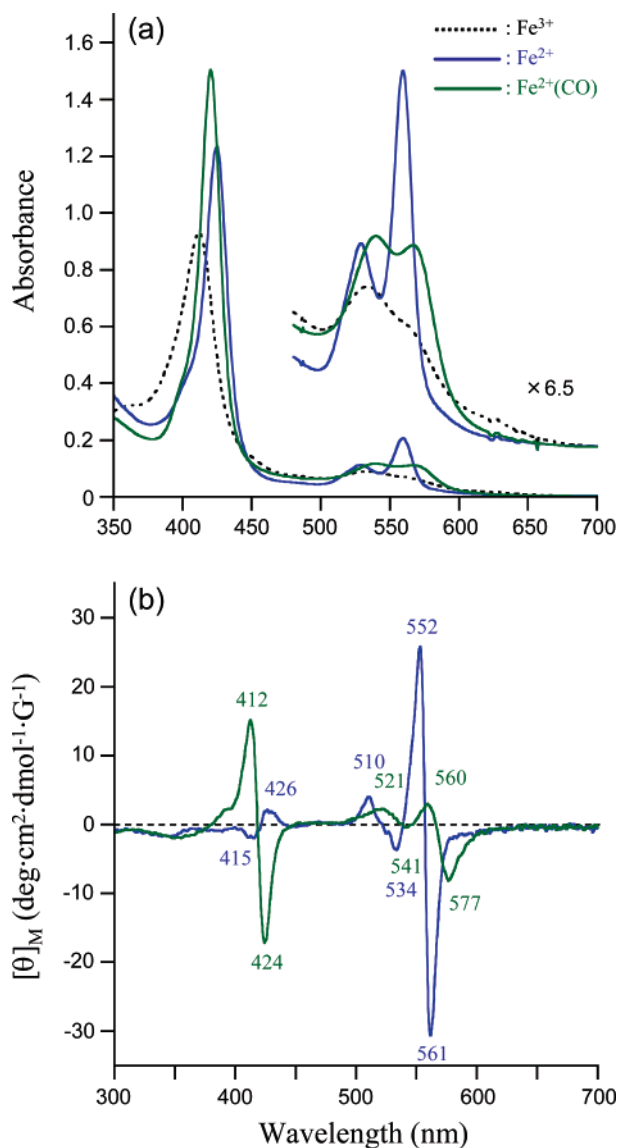


Figure 7. (a) UV-vis and (b) MCD spectral changes of rHSA(HF/R186H)-heme complex in 50 mM potassium phosphate buffered solution (pH 7.0, 22 °C).

hydrophobic amino acid (or substituent) around the O₂ binding site.^{13,14,17–19} We expected that increasing the hydrophobicity of the distal side of the heme pocket by insertion of a nonpolar residue would reduce the O₂ binding affinity of the rHSA-heme complex. The most suitable position for this introduction could be at Arg-186, which is the entrance of the heme pocket and is rather close to the central Fe²⁺ ion.

Thus, we designed new triple mutants rHSA(HL/R186L) and rHSA(HL/R186F) in an effort to prepare rHSA-based artificial hemoproteins having the same O₂ binding affinity as human RBC (Figure 9). An important structural factor in these mutants is Y161L, which is likely to allow rotation of the isopropyl group of Leu-185 above the O₂ coordination site.

MCD spectra in the Soret band region of ferric rHSA(HL/R186L)-hemin and rHSA(HL/R186F)-hemin both showed very low intensity, essentially the same as that observed for rHSA(HL)-hemin (Figure 8). The reduced ferrous form demonstrated the characteristic UV-vis absorption and MCD spectra of the five-N-coordinate high-spin complex under an Ar atmosphere (Table 1; Figure S3, Supporting Information).

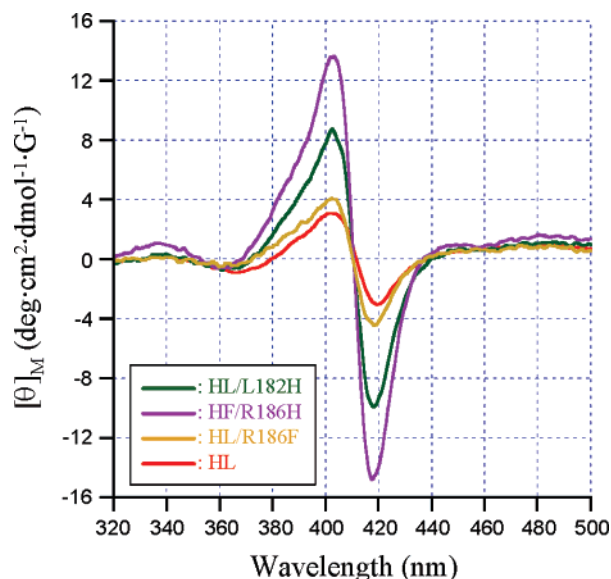


Figure 8. MCD spectra of rHSA(182-mutant)-hemin and rHSA(186-mutant)-hemin complexes in 50 mM potassium phosphate buffered solution (pH 7.0, 22 °C).

Upon bubbling of O₂ gas through the solutions, the spectral patterns were shifted to that of the O₂ adduct complex. The distinct features of all the spectra were quite similar to those of rHSA(HL)-heme.

Following laser flash photolysis, the absorption decays associated with O₂ recombination with rHSA(HL/R186L)-heme and rHSA(HL/R186F)-heme were monophasic, which suggests that the distal space in the pocket is uniform, in contrast to the L185N mutants. The kinetics for CO rebinding were still composed of double exponentials, consistent with the existence of two different geometries of the axial His-142 coordination to the central Fe²⁺ ion of the heme.

We previously showed that rHSA(HF) binds O₂ with significantly higher affinity than rHSA(HL) and reasoned that the presence of Leu rather than Phe at position 161 allowed a downward rotation of the adjacent L185 side chain that restricted access to the O₂ binding site on the heme group and reduced the affinity by a factor of 6 (Table 2).^{11b} Strikingly, however, insertion of Leu or Phe at position 186 in the presence of Leu-161 [as in rHSA(HL/R186L)-heme and rHSA(HL/R186F)-heme complexes] yielded $k_{on}^{O_2}$ and k_{on}^{CO} values that were 3–4-fold higher than those of rHSA(HL)-heme. The presence of a hydrophobic residue at position 186 may restrict the mobility of Leu-185 and thereby enhance access to the O₂ binding site (Figure 9).

Overall, the O₂ and CO binding parameters of rHSA(HL/R186L)-heme and rHSA(HL/R186F)-heme were more similar to those of rHSA(HF)-heme. In species I, for example, the k_{off}^{CO} values were almost identical, which again implies unhindered axial coordination structures of His-142 to the heme; as a result, the CO binding affinities of these triple mutants ($P_{1/2}^{CO}$ 0.0010–0.0018 Torr) were close to that of the rHSA(HF)-heme complex. In contrast, the O₂ dissociation rate constants of rHSA(HL/R186L)-heme and rHSA(HL/R186F)-heme were 3–4-fold higher than found for rHSA(HF)-heme, which modestly reduced the O₂ binding affinities (higher $P_{1/2}^{O_2}$). This could be due to the increase in the hydrophobicity in the distal pocket. Crucially, the O₂ binding affinities of rHSA(HL/

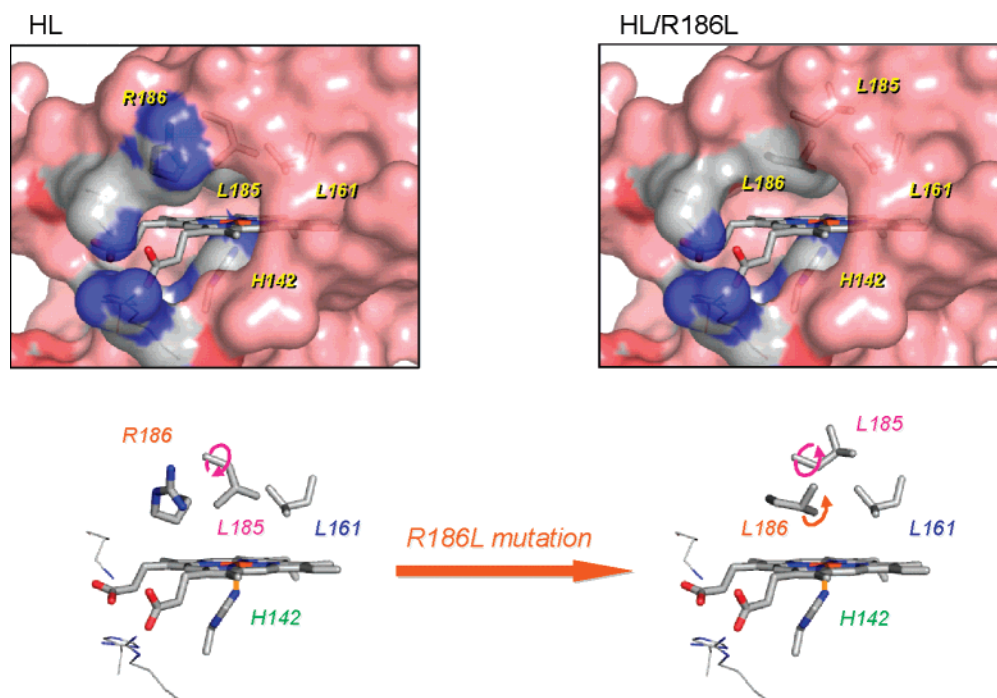
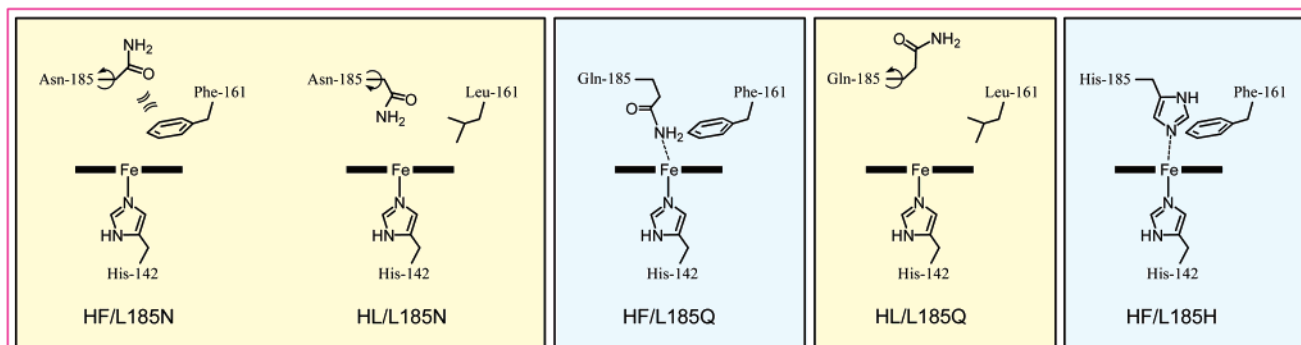
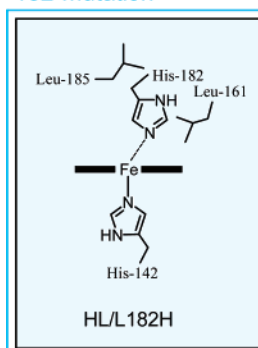


Figure 9. Structural models of rHSA(HL)–heme and rHSA(HL/R186L)–heme complexes. Introduction of R186L mutation may induce upward rotation of the L185 residue.

185-mutations



182-mutation



186-mutations

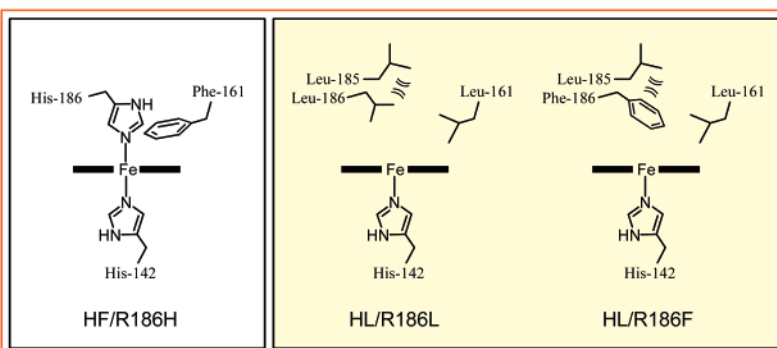


Figure 10. Schematic illustrations of the engineered distal amino acids in the heme pocket of rHSA(triple mutant)–heme: (yellow) five-coordinate high-spin ferrous complex; (blue) five-coordinate high-spin complex including six-coordinate low-spin ferrous complex; (pink) six-coordinate low-spin ferrous complex.

R186L)–heme ($P_{1/2}^{O_2}$ 10 Torr) and rHSA(HL/R186F)–heme ($P_{1/2}^{O_2}$ 9 Torr) are essentially indistinguishable from that of human RBC ($P_{1/2}^{O_2}$ 8 Torr). These results show that there are several different combinations of mutations that can confer the RBC-like O_2 binding affinity to the prosthetic heme group.

Another possibility, yet to be explored, is that insertion of a proximal His into the 186 position would construct a distal pocket on the opposite side of the porphyrin plane (the Ile-142 side), that would provide somewhat different O_2 binding properties of the heme.

Conclusions

Transport of O₂ by rHSA–heme complexes could be of great clinical importance, not only as a blood alternative but also as an O₂-providing therapeutic fluid. Such a synthetic compound has the potential advantage of not having to be matched to the recipient's blood type; moreover, it could be prepared in controlled facilities without viral contamination.

We have previously demonstrated that rHSA–heme complexes can be engineered to bind O₂ reversibly;¹¹ however, these complexes did not display optimal O₂ binding affinities. By use of structure-based mutagenesis of HSA combined with chemical modification of the synthetic iron–porphyrin, we have attempted to modify the heme pocket architecture so as to refine the O₂ binding properties of rHSA–heme complexes. By focusing on modifications on the distal side of the heme binding pocket in rHSA, we have successfully engineered distinct rHSA(triple mutant)–heme complexes with a broad range of O₂ binding affinities. Schematic illustrations of the engineered distal amino acids in the heme pocket of the different rHSA mutants are shown in Figure 10. These include mutants such as rHSA(HL/L185N) with affinities that mimic the high affinity of Hb(α) ($P_{1/2}^{O_2}$ 0.24 Torr) and others [e.g., rHSA(HL/R186L)] with affinities similar to that of human RBC ($P_{1/2}^{O_2}$ 8 Torr).

The highest affinity mutants rHSA(HL/L185N) and rHSA(HF/L185N) both contain Asn-185, which has a short amide side chain that significantly enhances the O₂ binding affinity, particularly when the neighboring amino acid is Leu-161. The N–H bond of the Asn-185 may face the terminal oxygen atom of the Fe–O₂ moiety, providing an amide dipole that stabilizes the O₂ binding to the heme. This interpretation is consistent with the findings of Chang et al.,³⁶ who first demonstrated that the dipole–dipole interaction between the Fe–O₂ and amide group can produce kinetic and thermodynamic control of the dioxygenation of the model hemes. In contrast, introduction of the larger Gln and His side chains at position 185 partly provided a six-coordinate heme character and therefore did not stabilize O₂ binding.

In a different approach, substitution of the polar Arg-186 at the entrance of the heme pocket with Leu or Phe caused a useful reduction in the O₂ binding affinity, yielding $P_{1/2}^{O_2}$ values that are very close to that of the human RBC and therefore well adapted for O₂ transport in vivo (Table 2). The impact of these substitutions may be due to their interaction with the adjacent residue, L185, which results in enhanced access to the O₂ binding site.

(36) Chang, C. K.; Ward, B.; Young, R.; Kondylis, M. P. *J. Macromol. Sci., Chem.* **1988**, A25, 1307–1326.

Other mutations were deleterious to O₂ binding but nevertheless produced complexes that might have other uses. For example, rHSA(HF/R186H)–heme formed a typical bis-histidyl Fe³⁺ or Fe²⁺ complex. In the circulation, free heme is known to participate in the Fenton reaction to produce the highly toxic hydroxyl radical. However, it is sequestered by Hpx, in which the bis-histidyl coordination tightly fixes the heme with the highest binding affinity of any known protein.^{1,2} In the same manner, rHSA(HF/R186H) has a bis-histidine clamp for heme and might conceivably be exploited as an antioxidant reagent to protect the body from oxidative damage after blood heme overload.

On the other hand, it would be of great importance to study the NO binding property of rHSA(mutant)–heme for practical medical applications. Some of the Hb-based blood substitutes leak through the vascular endothelium and capture the endothelial-derived relaxing factor, NO, that elicits an acute increase in blood pressure by vasoconstriction.³⁷ Our rHSA(mutant)–heme would bind NO in the same way as Hb, but it would not induce such hypertension, because the albumin carrier has low permeability through the muscle capillary pore.³⁸

Ultimately, to fully understand the structural basis of the effects of the various mutations on O₂ binding, it will be necessary to examine the structural details of the heme binding pocket. Crystal structural analysis of the rHSA(mutant)–heme complexes is now underway. Structural information should enhance our ability to design mutations that will further optimize the O₂ binding properties of these complexes.

Acknowledgment. This work was supported by PRESTO “Control of Structure and Functions”, JST, Grant-in-Aid for Scientific Research (16350093) from JSPS, and by Health Science Research Grants (Regulatory Science) from MHLW Japan. The work at Imperial College London was partially carried out as the Japan–U.K. Research Cooperative Program (Joint Project) of JSPS.

Supporting Information Available: UV–Visible absorption and MCD spectra of rHSA(HL/L185Q)–heme, absorption decay of O₂ rebinding to rHSA(HL/L185N)–heme after laser flash photolysis, and MCD spectra of rHSA(HL/R186F)–heme complex. This material is available free of charge via the Internet at <http://pubs.acs.org>.

JA074179Q

(37) Squires, J. E. *Science* **2002**, 295, 1002–1005.

(38) Tsuchida, E.; Komatsu, T.; Matsukawa, Y.; Nakagawa, A.; Sakai, H.; Kobayashi, K.; Suematsu, M. *J. Biomed. Mater. Res.* **2003**, 64A, 257–261.